Generated Pattern Current for Electroplating and Electrochemical Etching: Diffusion Layer Control, Grain Nucleation Engineering, and Dendrite Suppression

Ibrahim Karakoc

GigaPulse Energy, Izmir, Turkey | ibrahim@gigapulse.energy

PCT/TR2025/051176 | USPTO Appl. No. 19/298,223 | Priority Date: July 23, 2025

Abstract

Electroplating and electrochemical etching are current-controlled surface processes in which plating quality—grain size, surface roughness, dendrite formation, and coating uniformity—is determined by the interplay of three concurrent physical phenomena: diffusion layer ion transport, grain nucleation kinetics, and surface morphology evolution. Conventional direct current (DC) plating applies a constant current density that simultaneously saturates the diffusion layer, drives uncontrolled grain growth, and creates conditions favorable for dendrite formation. Pulse plating improves upon DC through periodic off-intervals but uses fixed duty cycles and frequencies that do not adapt to evolving surface conditions.

This paper presents the application of the Generated Pattern Current (GPC) paradigm, implemented through the Dynamic Defined Pattern Charging (DDPC) framework, to electroplating and electrochemical etching. GPC independently controls diffusion layer replenishment through timed low-current relaxation intervals, grain nucleation density through high-overpotential pulse sequences, and dendrite suppression through periodic interruption of local current density feedback loops. Theoretical analysis of Butler-Volmer kinetics, Fick's diffusion law, and nucleation theory predicts 30–50% reduction in surface roughness, significant grain refinement, complete dendrite suppression, and improved coating uniformity compared to DC plating at equal average current density. The GigaPulse Lab platform provides a reference implementation with closed-loop real-time impedance monitoring and adaptive pattern execution for production plating lines.

Keywords: Generated Pattern Current (GPC); Dynamic Defined Pattern Charging (DDPC); electroplating; pulse plating; electrochemical etching; diffusion layer; grain nucleation; dendrite suppression; Butler-Volmer kinetics; surface morphology; electrodeposition

1. Introduction

1.1 The Electroplating Quality Problem

Electroplating is one of the oldest and most widely deployed electrochemical manufacturing processes, with applications spanning semiconductor interconnect fabrication, printed circuit board production, automotive surface protection, aerospace corrosion resistance, and decorative finishing [2,3]. The global electroplating market exceeds $15 billion annually, with

coating quality—uniformity, grain structure, adhesion, and surface roughness—directly determining product performance and service life [4].

The quality of an electrodeposited coating is governed by the interplay of three concurrent physical processes during deposition. First, ion transport through the diffusion boundary layer determines the local metal ion concentration at the electrode surface and sets the upper limit on sustainable current density [5,6]. Second, the competition between nucleation and growth at the electrode surface determines the grain size and crystal structure of the deposit [7,8]. Third, the feedback between local current density and surface topology drives either stable, uniform deposition or unstable dendrite formation [10,11]. Under conventional DC plating, these three processes are driven by the same constant current density and cannot be independently optimized.

1.2 Limitations of DC and Pulse Plating

DC plating applies a constant current density J_DC throughout deposition. As metal ions are reduced at the electrode surface, the local ion concentration C_s decreases below the bulk concentration C_0, establishing a concentration gradient within the diffusion layer of thickness δ. When J approaches the limiting current density J_lim = nFDC_0/δ, ion transport becomes the rate-limiting step, surface concentration approaches zero, and deposit quality degrades sharply—producing rough, porous, or burnt deposits [5,22].

Pulse plating was developed to address diffusion layer depletion by introducing periodic off-intervals during which ion transport replenishes the surface concentration [7,8,9]. However, conventional pulse plating is defined by fixed duty cycle and fixed frequency parameters that do not adapt to the evolving state of the electrode surface. The off-time provides diffusion replenishment but does not control nucleation kinetics independently of replenishment. The on-time current density and duration determine both grain nucleation and the resumption of diffusion depletion simultaneously. Pulse reverse plating adds a cathodic-to-anodic reversal that dissolves high-current-density protrusions but introduces additional complexity and potential for substrate attack [18].

The fundamental limitation of both DC and fixed-parameter pulse plating is that the temporal structure of the current is not treated as a design variable. GPC addresses this by designing the temporal current profile to independently target each of the three concurrent physical processes at their characteristic timescales.

1.3 GPC as Temporal Current Design for Electrodeposition

Generated Pattern Current (GPC) is defined and protected under PCT/TR2025/051176 and USPTO Application No. 19/298,223 (priority date July 23, 2025) [1]. The theoretical foundation derives from Jensen's inequality applied to the nonlinear Butler-Volmer kinetics and nucleation rate equations governing electrodeposition: the response of a nonlinear electrochemical system to a temporally structured current I(t) is not equal to the response to the time-averaged constant current $\bar{I}$:

$$f(\bar{I}) \neq \langle f(I(t)) \rangle$$

where f represents any nonlinear response—nucleation rate, grain growth rate, or local surface concentration. Faraday's law guarantees that the total mass deposited depends only on the time-averaged current $\langle I(t) \rangle = \bar{I}$, so GPC preserves the deposition rate while changing the quality of the deposit through temporal current structure [5,22].

GPC has been applied across multiple electrochemical domains including battery formation [27], charging optimization [28], photovoltaic activation [29], fuel cell conditioning [30], hybrid capacitor activation [31], and semiconductor conditioning [32]. The unified theoretical framework is described in [26]. Electroplating represents perhaps the most natural GPC application domain because the entire process is already defined by current-controlled electrochemistry, and the three quality-determining processes—diffusion, nucleation, and morphology—each have distinct characteristic timescales accessible to temporal current design.

1.4 Scope

Section 2 presents the electrochemical physics of electrodeposition. Section 3 analyzes the three GPC control mechanisms. Section 4 describes protocol design including GigaPulse Lab implementation. Section 5 covers electrochemical etching. Section 6 quantifies expected outcomes. Section 7 presents the experimental validation framework. Section 8 discusses implications. Section 9 concludes.

2. Electroplating Physics

2.1 Faraday's Law and Deposition Rate Invariance

The total mass deposited m is governed by Faraday's law:

$$m = M \cdot \langle I \rangle \cdot t / (n \cdot F)$$

where M is the molar mass of the deposited metal [19], $\langle I \rangle$ is the time-averaged current, t is the deposition time, n is the number of electrons transferred per metal ion, and F is Faraday's constant [5]. This relation depends only on the time-averaged current—not on its temporal structure. GPC therefore preserves deposition rate identically to DC or pulse plating at the same average current density while modifying the quality-determining processes through temporal structure. This is a key property: GPC's benefits in coating quality come at zero cost to throughput.

2.2 Butler-Volmer Kinetics and Overpotential

The partial current density for metal reduction at the electrode surface is governed by Butler-Volmer kinetics [5]:

$$j = j_0 \, [\exp(\alpha F \eta / RT) - \exp(-(1-\alpha) F \eta / RT)]$$

where j_0 is the exchange current density, α is the transfer coefficient (typically 0.3–0.5), η is the overpotential, R is the gas constant, and T is temperature. The Butler-Volmer equation is strongly nonlinear in η. For cathodic overpotentials $|\eta| \gg RT/F$ (Tafel region), $j \propto$

exp(αF|η|/RT). This exponential nonlinearity means that Jensen's inequality applies directly: the time-averaged deposition current density under a structured overpotential waveform is not equal to the Butler-Volmer response at the time-averaged overpotential [5,23].

The practical implication is that the peak overpotential during a GPC high-current phase drives nucleation at a rate exponentially higher than the DC average overpotential, even though the average current density (and therefore the deposition rate) is identical. This is the mechanism by which GPC achieves fine-grained deposits without reducing throughput.

2.3 Diffusion Layer and Limiting Current Density

Metal ion transport from bulk electrolyte to the electrode surface occurs through a diffusion boundary layer of thickness δ, governed by Fick's first law [5,6]:

$$J_{diff} = nFD(C_0 - C_s) / \delta$$

where D is the ionic diffusion coefficient, C_0 is the bulk concentration, and C_s is the surface concentration. The limiting current density—the maximum sustainable deposition current before surface concentration reaches zero—is:

$$J_{lim} = nFDC_0 / \delta$$

Under DC plating at J approaching J_lim, C_s → 0, the overpotential increases sharply, and co-deposition of hydrogen and formation of burnt or powdery deposits occurs. The diffusion layer thickness δ under quiescent conditions scales as $\delta \propto (Dt)^{1/2}$, increasing with time as the surface is depleted. GPC's periodic low-current intervals allow C_s to recover toward C_0 through diffusion, reducing the effective time-averaged δ and maintaining J well below J_lim throughout the deposition [7,8].

2.4 Grain Nucleation Kinetics

Grain nucleation at the electrode surface follows classical nucleation theory, with the nucleation rate J_nuc governed by:

$$J_{nuc} \propto exp(-\Delta G^*/kT) , \Delta G^* \propto 1/\eta^2$$

where ΔG* is the free energy barrier for critical nucleus formation, which is inversely proportional to the square of the overpotential [3,20,23]. At high overpotential (large |η|), ΔG* is small and nucleation rate is very high—many small nuclei form. At low overpotential, ΔG* is large, nucleation is slow, and growth of existing nuclei dominates—producing large grains. DC plating at moderate overpotential produces an intermediate grain size determined by the fixed J_DC. GPC's high-current peaks drive |η| to high values during the nucleation phase, creating a high density of small nuclei. The subsequent growth phase at lower current density develops these nuclei into a fine-grained deposit [12,13,14].

2.5 Dendrite Formation Mechanism

Dendrite formation in electrodeposition arises from a positive feedback loop between local current density and surface topology [10,11]. A surface protrusion—arising from a statistical fluctuation in local deposition rate—experiences a higher local current density than the

surrounding flat surface because electric field lines concentrate at tips. This higher local current density drives faster deposition at the protrusion, increasing its height, further concentrating the field lines, and accelerating growth in a self-amplifying cycle. The feedback gain is proportional to J/J_lim: when J approaches J_lim, dendrite growth rate increases sharply [10,11].

GPC suppresses dendrite formation through two mechanisms. First, by maintaining C_s above the depletion threshold through diffusion relaxation intervals, J/J_lim is kept below the critical value for unstable growth. Second, the periodic low-current phases interrupt the positive feedback loop before it can amplify a nascent protrusion to dendritic dimensions. Each low-current interval resets the local current density distribution to near-uniform values, preventing the self-amplification that leads to dendrite growth.

3. Three GPC Control Mechanisms for Electrodeposition

3.1 Diffusion Layer Replenishment

The diffusion relaxation mechanism implements periodic reduction of the applied current to $I_{relax} = \alpha \cdot I_{dc}$ ($\alpha = 0.05–0.15$) for a controlled relaxation interval t_{relax}. During this interval, the depleted surface concentration C_s recovers toward the bulk value C_0 through Fickian diffusion:

$$\partial C/\partial t = D \cdot \partial^2 C/\partial x^2 \quad [relaxation\ phase]$$

The recovery time constant is $\tau_{diff} \sim \delta^2/D$. For typical aqueous electrolytes ($D \sim 10^{-9}$ m²/s, $\delta \sim 50–200$ μm), $\tau_{diff} \sim 2–40$ ms. GPC relaxation intervals of comparable duration restore C_s to near-bulk values before the next high-current deposition phase. The time-averaged surface concentration under GPC is substantially higher than under DC at the same average current density, allowing higher sustained current densities without approaching the limiting current condition [7,8,9].

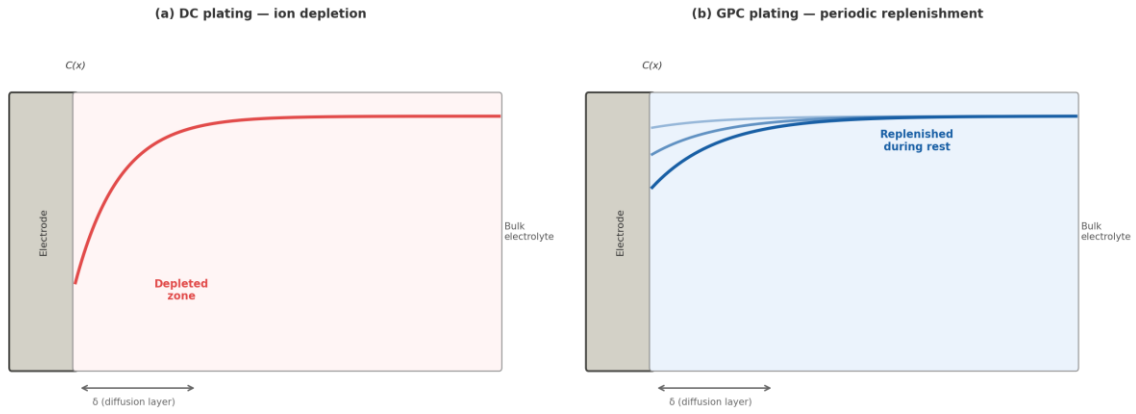

Figure 1. Diffusion layer dynamics: DC plating drives ion depletion near the electrode surface; GPC periodic low-current intervals allow ionic replenishment.

Figure 1. Diffusion layer dynamics: DC plating drives progressive ion depletion near the electrode surface; GPC periodic low-current relaxation intervals allow ionic replenishment, maintaining surface concentration above the depletion threshold.

3.2 Grain Nucleation Control Through Overpotential Pulse Shaping

The grain nucleation mechanism exploits the exponential dependence of nucleation rate on overpotential. GPC designs the current profile to separate the nucleation-dominant and growth-dominant phases:

During the high-current nucleation phase (I_peak, duration t_nuc), the overpotential is elevated to |η_peak|, driving J_nuc to high values and creating a dense population of small nuclei across the electrode surface. The critical nucleus radius r* = 2γV_m/(nF|η|) decreases with increasing |η|, so higher-overpotential nucleation produces smaller, more uniformly distributed nuclei [3,23].

During the growth phase (I_growth < I_peak, duration t_grow), the overpotential is reduced, suppressing new nucleation while allowing controlled growth of the existing nucleus population. The ratio t_nuc/t_grow controls the balance between nucleus density and grain size: short nucleation pulses followed by longer growth intervals produce the finest grain structure for a given target coating thickness.

This two-phase approach is fundamentally different from both DC plating (which cannot separate nucleation from growth timescales) and fixed-parameter pulse plating (which applies the same on-time current density to both nucleation and growth without independent control of each phase) [8,18].

3.3 Dendrite Suppression Through Feedback Interruption

GPC suppresses dendrite formation through the combined effect of diffusion replenishment and periodic current interruption. The critical condition for dendrite stability can be expressed through the Wagner number Wa:

$$Wa = \kappa \cdot (dj/d\eta)^{-1} \cdot L^{-1}$$

where κ is the electrolyte conductivity, dj/dη is the slope of the Butler-Volmer curve, and L is a characteristic electrode dimension. High Wa (>1) promotes uniform current distribution; low Wa (<1) promotes non-uniform distribution and dendrite-favorable conditions. GPC's relaxation intervals restore the electrolyte concentration uniformity that underpins high Wa, while the periodic current interruption resets any nascent protrusion's growth advantage before it can amplify to macroscopic scale [10,11].

Quantitatively, dendrite suppression requires that the time constant for protrusion growth be longer than the GPC pattern period. For copper electrodeposition (a common dendrite-prone system), protrusion growth rates under near-limiting conditions are on the order of micrometers per second, while GPC pattern periods of 10–100 ms are sufficient to interrupt the feedback cycle before dendrites reach problematic dimensions [10].

Figure 2. Grain structure and surface morphology: DC (coarse grain, dendrites), pulse (medium grain), GPC (fine-grained, smooth, dendrite-free). Schematic cross-sections.

Figure 2. Grain structure and surface morphology comparison: (a) DC plating produces coarse grains and dendrites; (b) pulse plating yields medium grain size with reduced dendrites; (c) GPC produces fine-grained, smooth, dendrite-free deposits. Schematic cross-sections.

4. GPC Electroplating Protocol Design

4.1 Three-Phase Pattern Architecture

The GPC electroplating protocol integrates the three mechanisms into a composite three-phase current profile:

> *I(t) = I_nuc [nucleation phase, t_nuc] → I_grow [growth phase, t_grow] → I_relax [relaxation phase, t_relax]*

The time-average constraint ⟨I(t)⟩ = I_dc is satisfied by design: I_nuc·t_nuc + I_grow·t_grow + I_relax·t_relax = I_dc·(t_nuc + t_grow + t_relax). Parameter selection proceeds from characterization of the target plating system: the diffusion layer time constant τ_diff from rotating disk electrode (RDE) measurements sets t_relax; the target grain size sets the nucleation pulse amplitude I_nuc through the nucleation rate equation; and the coating thickness target sets the total deposition time.

Unlike pulse plating, where duty cycle and frequency are fixed inputs, GPC parameters can be adapted in real time based on the evolving electrode state. The GigaPulse Lab platform provides closed-loop feedback from real-time electrochemical impedance spectroscopy: the charge transfer resistance R_ct and double-layer capacitance C_dl extracted from impedance data reflect the instantaneous state of the electrode surface and can be used to adaptively adjust I_nuc and t_relax during deposition.

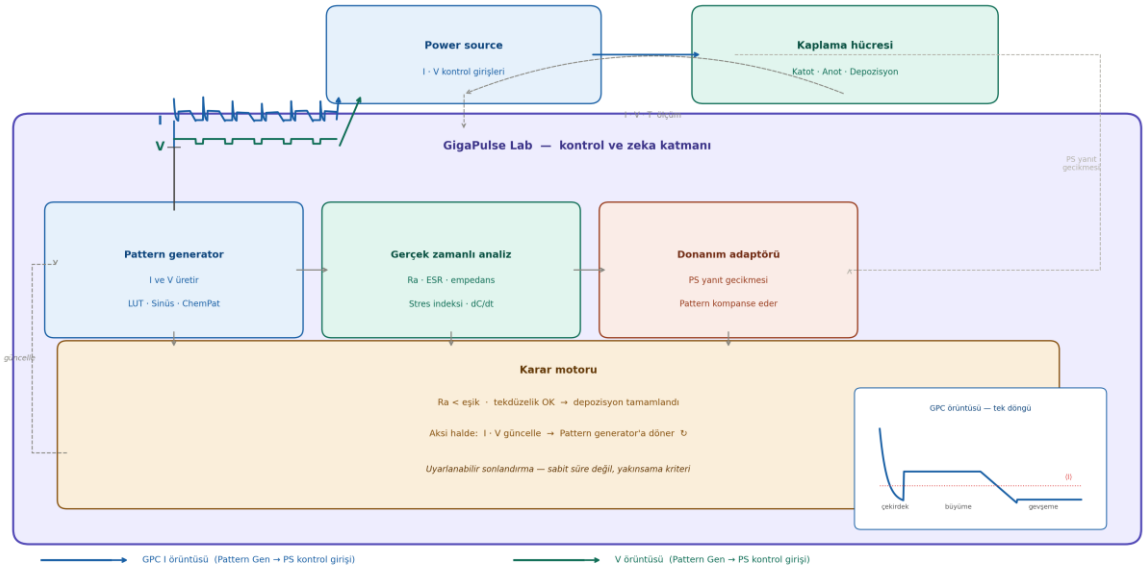

Figure 4. GPC tabanlı sistem mimarisi. GP Lab, Power Source'un I ve V kontrol girişlerine bağlanır — güç kaynağı değiştirilmez. GPC örüntü sinyalleri Pattern Generator'dan çıkar. Gerçek zamanlı geri besleme (I, V, T) kapalı döngü kontrolü sağlar.

Figure 4. GPC-based system architecture. GP Lab connects to the Power Source I and V control input terminals — no hardware replacement required. GPC pattern signals exit the Pattern Generator. Real-time feedback (I, V, T) enables closed-loop deposition control.

4.2 GigaPulse Lab Reference Implementation

The GigaPulse Lab platform serves as the reference implementation for GPC electroplating. GP Lab connects to the input terminals of the plating power supply and generates I and V control signals; the power supply applies the actual current to the plating cell. Real-time feedback—measured current, voltage, and cell impedance—returns to GP Lab for closed-loop control. The platform's full pattern library—Sinusoidal, SuperPulse, Gaussian, ChemPat, and custom LUT profiles—covers the range of electrodeposition applications from fine-pitch semiconductor interconnect to thick decorative coatings.

Application-specific calibration files encode the system-specific parameters for each plating chemistry and substrate type. For semiconductor copper interconnect damascene plating—where grain size, resistivity, and electromigration resistance of the deposited copper are critical—GPC calibration files incorporate the known superconformal filling additives' interaction with temporal current structure [13,14,16,17]. For automotive zinc-nickel alloy plating—where coating uniformity and porosity are the critical quality metrics—GPC files are calibrated for alloy composition control through differential nucleation kinetics of the two metals.

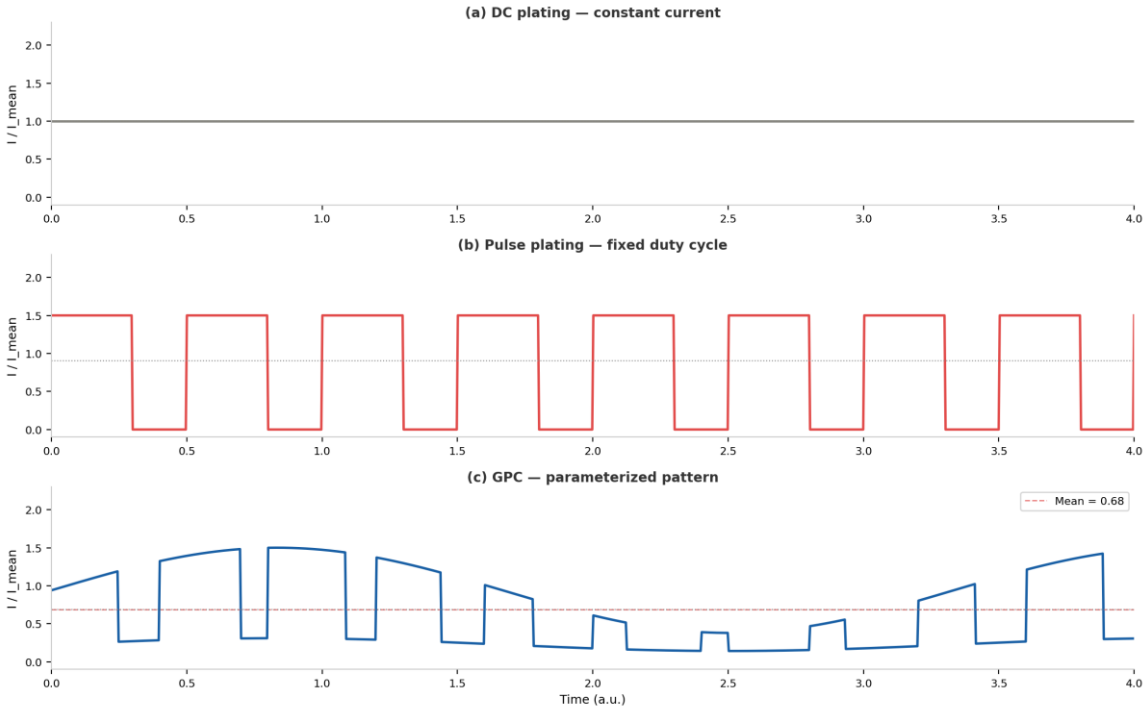

Figure 3. Current profile comparison: DC (constant), pulse plating (fixed duty cycle), and GPC (parameterized adaptive pattern). All profiles share the same mean current density.

Figure 3. Current profile comparison: (a) DC plating (constant current), (b) pulse plating (fixed duty cycle), (c) GPC (parameterized adaptive pattern with three-phase structure). All profiles share the same mean current density ⟨I⟩.

5. Electrochemical Etching

Electrochemical etching is the anodic dissolution analog of electroplating: M → M^(z+) + ze⁻. The same physical framework applies in reverse. The three critical quality metrics in etching are material removal rate uniformity, surface finish (controlled roughness), and selectivity (preferential etching of target features over substrate). Under DC anodic dissolution, the same diffusion layer, nucleation/dissolution kinetics, and surface feedback mechanisms that govern plating quality apply, but in reverse [24,25].

GPC controls electrochemical etching through three mechanisms analogous to those for plating. Diffusion relaxation intervals allow reaction products (dissolved metal ions) to diffuse away from the surface before they reach saturation concentrations that would slow dissolution and cause surface passivation. Dissolution pulse shaping controls the instantaneous dissolution overpotential, enabling selective activation of crystallographic planes with different dissolution rates—a mechanism exploited in electrochemical microfabrication for high-aspect-ratio feature etching [21]. Periodic current interruption prevents the runaway dissolution that leads to pitting and surface roughness amplification through the same positive feedback mechanism that drives dendrite formation in plating.

Electrochemical microfabrication applications—MEMS fabrication, through-silicon via formation, printed circuit board etching—require feature-scale uniformity and controlled sidewall angle that DC etching cannot achieve without complex electrolyte additive systems.

GPC temporal control provides an independent handle on etching uniformity without changing the electrolyte chemistry, enabling cleaner processes for semiconductor manufacturing.

6. Expected Outcomes

The quantitative predictions for GPC electroplating follow from the governing equations analyzed in Sections 2 and 3. The GPC quality improvement factor is defined separately for each metric:

$$\Psi_{GP,Ra} = Ra_{DC} / Ra_{GPC} \text{ (surface roughness reduction)}$$

$$\Psi_{GP,d} = d_{DC} / d_{GPC} \text{ (grain size reduction)}$$

Parameter	DC plating	Pulse plating	GPC plating
Surface roughness Ra	Reference	↓ 10–20%	↓ 30–50%
Grain size	Coarse	Medium	Fine-grained
Dendrite formation	Present	Reduced	Suppressed
Coating uniformity	Reference	Improved	↑ Further improved
Current efficiency	Reference	~Equal	↑ Increased
Deposition rate	Reference	~Equal	Preserved (same ⟨I⟩)
Adaptive control	None	Limited	Closed-loop feedback

Table 1. Predicted electroplating outcomes of GPC protocol compared to DC and pulse plating baselines at equal average current density.

7. Experimental Validation Framework

7.1 Proposed Protocol

Independent experimental validation requires parallel comparison of DC, pulse, and GPC plating protocols applied to identical substrate-electrolyte systems with equal average current density and total deposition time. The primary measurement suite includes: surface roughness Ra from contact or optical profilometry; grain size from SEM cross-section imaging and XRD peak broadening analysis (Scherrer equation); coating thickness uniformity from cross-sectional SEM at multiple locations; current efficiency from gravimetric measurement of actual versus theoretical mass deposited; and visual dendrite assessment at magnification.

A particularly informative validation format is copper electrodeposition from sulfate electrolyte, which is a well-characterized model system with known DC and pulse plating behavior and extensive literature baseline data [13,14,15,16]. Copper is highly prone to dendrite formation at current densities approaching J_{lim}, making dendrite suppression quantitatively testable. Grain size measurement by XRD is straightforward for copper and provides a direct quantitative metric for the nucleation control mechanism.

7.2 Application-Specific Validation Targets

For semiconductor damascene copper interconnect, the critical validation metrics are: grain size after deposition and post-anneal recrystallization (target: large bamboo-grained structure for electromigration resistance), resistivity (target: approaching bulk copper $\rho = 1.7\ \mu\Omega\cdot cm$), and superconformal fill of submicrometer features without seam or void defects [13,14]. GPC calibration files for this application incorporate the known interactions between temporal current structure and the suppressor/accelerator/leveler additive system used in damascene copper [16,17].

For automotive zinc-nickel alloy plating, validation metrics include: alloy composition uniformity across the plated surface (target Ni content 12–15 wt%), porosity from neutral salt spray testing, and adhesion strength. GPC enables alloy composition control through differential pulsing that exploits the different reduction potentials and diffusion coefficients of Zn^{2+} and Ni^{2+} ions [12,18].

8. Discussion

8.1 GPC vs Pulse Reverse Plating

Pulse reverse plating (PRP) combines forward cathodic pulses with brief anodic reversal pulses that selectively dissolve deposit protrusions, providing an alternative approach to surface leveling [18]. PRP effectively suppresses surface roughness and dendrite formation but introduces the risk of substrate attack during the anodic phase, particularly for complex geometries where the anodic current density may be unevenly distributed. PRP also adds electrolyte complexity for alloy plating systems where anodic dissolution selectivity differs between the deposited metals.

GPC achieves equivalent or superior surface leveling through purely cathodic operation: diffusion relaxation intervals suppress protrusion growth without anodic dissolution, eliminating substrate attack risk. The two approaches are complementary: GPC's diffusion relaxation mechanism and PRP's anodic dissolution mechanism address dendrite suppression through different physical pathways. Combined GPC+PRP protocols that use GPC-structured forward pulses with PRP-style anodic cleanup steps represent a natural extension that is supported by the GigaPulse Lab LUT pattern capability.

8.2 Industrial Deployment

Industrial deployment of GPC electroplating does not require replacement of the existing power supply. GP Lab connects to the I and V control input terminals of the existing DC or pulse plating power supply and generates GPC pattern signals; the power supply applies these signals to the plating cell. For new installations, the GP Lab integration is direct. For existing plating lines, retrofit is feasible through the GP Lab's power supply input terminal connection without modification of the plating cell, electrolyte system, or process chemistry. The energy cost of GPC plating is not significantly different from DC plating at the same average current, since Faraday's law guarantees equal total charge transfer for equal deposition.

9. Conclusion

This paper has established the theoretical framework for applying Generated Pattern Current to electroplating and electrochemical etching. The fundamental limitation of DC plating—that constant current density cannot independently control diffusion layer replenishment, grain nucleation, and dendrite suppression—is overcome by GPC's three-phase temporal current design. Jensen's inequality applied to Butler-Volmer kinetics and nucleation theory formally establishes that the response to structured temporal current differs from the response to its time-averaged equivalent, while Faraday's law guarantees that deposition rate is preserved.

The three GPC mechanisms—diffusion relaxation intervals, overpotential pulse shaping for nucleation control, and feedback interruption for dendrite suppression—operate at different timescales (milliseconds for nucleation, tens of milliseconds for diffusion, seconds for growth) and can be independently parameterized within a single composite current profile. Predictions include 30–50% surface roughness reduction, fine-grained deposits, complete dendrite suppression, and improved coating uniformity at equal average current density and throughput.

Electroplating is perhaps the most natural GPC application domain: the process is entirely current-controlled, all quality-determining phenomena are directly responsive to current temporal structure, and Faraday's law guarantees throughput invariance. The GigaPulse Lab platform provides immediate deployment capability on existing production plating lines.

[1] I. Karakoc, "Dynamic Defined Pattern Charging (DDPC)," PCT/TR2025/051176; USPTO Application No. 19/298,223. Priority Date: July 23, 2025.

[2] M. Schlesinger and M. Paunovic, Modern Electroplating, 5th ed., Wiley, 2010.

[3] M. Paunovic and M. Schlesinger, Fundamentals of Electrochemical Deposition, 2nd ed., Wiley, 2006.

[4] J. W. Dini, Electrodeposition: The Materials Science of Coatings and Substrates, Noyes, 1993.

[5] A. J. Bard and L. R. Faulkner, Electrochemical Methods: Fundamentals and Applications, 2nd ed., Wiley, 2001.

[6] J. O. Dukovic, "Feature-Scale Simulation of Resistive Electrolyte Deposits," IBM J. Res. Dev., vol. 37, pp. 125–141, 1993.

[7] N. Ibl, "Some Theoretical Aspects of Pulse Electrolysis," Surface Technol., vol. 10, pp. 81–104, 1980.

[8] J. C. Puippe and F. Leaman, Theory and Practice of Pulse Plating, AESF, 1986.

[9] M. S. Chandrasekar and M. Pushpavanam, "Pulse and Pulse Reverse Plating — Conceptual, Advantages and Applications," Electrochim. Acta, vol. 53, pp. 3313–3322, 2008.

[10] K. I. Popov, S. S. Djokic, and B. N. Grgur, Fundamental Aspects of Electrometallurgy, Kluwer Academic, 2002.

[11] D. P. Barkey, R. H. Muller, and C. W. Tobias, "Roughness Development in Metal Electrodeposition II: Stability Theory," J. Electrochem. Soc., vol. 136, pp. 2207–2214, 1989.

[12] T. Osaka, T. Homma, T. Yokoshima, and H. Yamazaki, "Electrodeposition of Soft Magnetic CoNiFe Thin Films," J. Electrochem. Soc., vol. 149, pp. C573–C578, 2002.

[13] P. C. Andricacos, C. Uzoh, J. O. Dukovic, J. Horkans, and H. Deligianni, "Damascene Copper Electroplating for Chip Interconnections," IBM J. Res. Dev., vol. 42, pp. 567–574, 1998.

[14] T. P. Moffat, D. Wheeler, and D. Josell, “Superconformal Electrodeposition of Copper,” Electrochem. Solid-State Lett., vol. 4, pp. C26–C29, 2001.

[15] D. Josell, D. Wheeler, W. H. Huber, and T. P. Moffat, “Superconformal Electrodeposition in Submicron Features,” Phys. Rev. Lett., vol. 87, p. 016102, 2001.

[16] R. Akolkar and U. Landau, “A Time-Dependent Transport-Kinetics Model for Additive Interactions in Copper Interconnect Metallization,” J. Electrochem. Soc., vol. 151, pp. C702–C711, 2004.

[17] K. R. Hebert, “Role of Chloride Ions in Suppression of Copper Electrodeposition by Polyethylene Glycol,” J. Electrochem. Soc., vol. 152, pp. C283–C287, 2005.

[18] E. J. Podlaha and D. Landolt, “Pulse-Reversal Plating of Nanostructured NiFe Alloys,” J. Electrochem. Soc., vol. 144, pp. L200–L202, 1997.

[19] J. Newman and K. E. Thomas-Alyea, Electrochemical Systems, 3rd ed., Wiley, 2004.

[20] R. Winand, “Electrodeposition of Metals and Alloys: New Results and Perspectives,” Electrochim. Acta, vol. 39, pp. 1091–1105, 1994.

[21] M. Datta and D. Landolt, “Fundamental Aspects and Applications of Electrochemical Microfabrication,” Electrochim. Acta, vol. 45, pp. 2535–2558, 2000.

[22] C. T. J. Low, R. G. A. Wills, and F. C. Walsh, “Electrodeposition of Composite Coatings Containing Nanoparticles in a Metal Deposit,” Surf. Coat. Technol., vol. 201, pp. 371–383, 2006.

[23] Y. D. Gamburg and G. Zangari, Theory and Practice of Metal Electrodeposition, Springer, 2011.

[24] S. Armyanov, “Crystalline Structure and Magnetic Properties of Electrodeposited Alloys,” Electrochim. Acta, vol. 45, pp. 3901–3912, 2000.

[25] N. Ibl and H. Suggs, “Diffusion-Layer Control in Electroplating,” J. Electrochem. Soc., vol. 124, pp. 1799–1806, 1977.

[26] I. Karakoc, “Generated Pattern Current (GPC): A Unified Framework for Temporal Energy Structuring in Electrochemical Systems,” SSRN 6387818, 2026.

[27] I. Karakoc, “Generated Pattern Current for Lithium-Ion Battery Formation,” SSRN 6392399, 2026.

[28] I. Karakoc, “Generated Pattern Current for Lithium-Ion Battery Charging Optimization,” SSRN 6392719, 2026.

[29] I. Karakoc, “Generated Pattern Current for Photovoltaic Cell and Module Activation,” SSRN 6426418, 2026.

[30] I. Karakoc, “Generated Pattern Current for PEM Fuel Cell MEA Conditioning,” SSRN 6427558, 2026.

[31] I. Karakoc, “Generated Pattern Current for Hybrid Capacitor Production Activation,” SSRN 6431938, 2026.

[32] I. Karakoc, “Generated Pattern Current for Power Semiconductor Device Conditioning,” SSRN 6437961, 2026.

References

Acknowledgments

The GPC-based electroplating and etching protocol is protected under PCT/TR2025/051176 and USPTO Application No. 19/298,223. The author is the named inventor. No external funding was received for the preparation of this manuscript.

Declaration of Competing Interest

Ibrahim Karakoc holds intellectual property and commercial rights related to the Generated Pattern Current (GPC) and Dynamic Defined Pattern Charging (DDPC) technology described in this paper through GigaPulse Energy, Izmir, Turkey.

Data Availability

Data will be made available on request.

Declaration on the Use of AI Writing Assistance

The author used AI-assisted writing tools for language editing and manuscript preparation. The scientific content, theoretical analysis, and all intellectual contributions are entirely the work of the author. The author takes full responsibility for the integrity of the work.